

## Design of a double-stator linear switched reluctance motor for shunting railway channels

El Manâa BARHOUMI\*, Mansour HAJJI, Boujemâa Ben SALAH

National Engineering School of Tunis, University of Tunis El Manar, Tunis, Tunisia

Received: 19.07.2012 • Accepted: 04.11.2012 • Published Online: 17.01.2014 • Printed: 14.02.2014

**Abstract:** This paper presents the design and modeling of a double-stator linear switched reluctance motor for motorizing a railway channels' shunting system. The magnetic behavior of this actuator is nonlinear due to the saturation and nonlinear magnetization curves of the materials used in this actuator. For this reason, the electromagnetic quantities such as force, flux linkage, and inductance are calculated with the finite element method using the Maxwell tool. The obtained results are presented and discussed. In order to elaborate some control strategies, a new model for the proposed actuator, based on the flux and force characteristics, is validated by the simulation results using MATLAB/Simulink.

**Key words:** Shunting system, railway channel, double stator linear switched reluctance motor, finite element analysis, force, flux, inductance, modeling

### 1. Introduction

Nowadays, the shunting systems of railway channels use a rotating motor coupled with a system for movement transformation (rotary to linear). This electromechanical system is able to stall, lock, and control the blades of rail track switches. However, the currently used entrainment system is very complicated and expensive.

To improve the performances and reduce the cost of the shunting system, a linear switched reluctance motor (LSRM) can be used in this industrial application. Moreover, the simple structure of the LSRM added to the robustness and high power densities have made it more attractive for many industrial applications during the last decade [1]. The LSRM's reliability is quite improved compared with the other electric motors used in positioning applications [2,3]. Indeed, no magnet is installed in the LSRM structure and no copper winding is installed on the mobile part.

The LSRM develops a linear step movement with high precision, and this advantage allows it to become popular in linear industrial drives. Each electrical pulse results in a discrete incremental linear movement called a step [4]. The LSRM offers a solution for applications requiring high-position precision. Hence, LSRMs have been used in applications requiring precise motion control, such as propulsion systems for vertical elevator and electrical syringes.

In order to generate a high-propulsion force, the LSRM must be operated in the saturation zone. In saturation conditions, the principal magnetic characteristics, such as the flux linkage and the propulsion force, are highly nonlinear. Consequently, the analytical methods based on some hypotheses are not very accurate to compute the electromagnetic characteristics of these electrical machines [5,6]. With the aim of overcoming

\*Correspondence: [elmanaabarhoumi@isetkr.rnu.tn](mailto:elmanaabarhoumi@isetkr.rnu.tn)

the limitations of analytical methods, numerical methods, such as finite element analysis (FEA), are preferred in most cases for the design and modeling of electrical machines. Moreover, the finite element method (FEM) provides good agreement with the experimental results.

This paper is organized as follows. The description of the shunting system used for the railway channels is presented in Section 2. Section 3 is on the analytical and FEM design of the new motorization for shunting railway channels. The flux and force characteristics calculated using the FEM are presented and discussed in Section 4. Section 5 is reserved for modeling of the double-stator LSRM using the results obtained with the FEM. In Section 6, based on electromagnetic curves, the MATLAB/Simulink model is built and simulation tests are carried out. Finally, Section 7 presents our conclusions and perspective.

## 2. Presentation of the shunting system

To guide a train in a direction between 2 tracks, a mechanical system is installed at each railway junction. This system is composed of 2 railway channels with an intermediate junction for switching the train's direction. Figure 1 shows that the intermediate junction is positioned so that the train is pointing to the right. In order to change the direction of the displacement so the train will be guided to the left track, a mechanism is provided to move the switcher from the 1st position to the 2nd one. This operation requires a lever to be moved, which is now operated by a controlled electric motor [6,7]. Currently, an asynchronous motor coupled with a transformation system of movement is installed in the entrainment system for shunting the railway channels. This electromechanical system can stall, lock, and control the blades of the rail track switches. The currently used entrainment system for shunting railway channels is presented in Figure 2. However, this system with a control and power supply is complicated and very expensive. Hence, to ameliorate the shunting system reliability, the proposed research work carried out in this paper consists of the design and analysis of a new motorization based on the use of a LSRM. Moreover, for moving the switch, a linear movement is necessary and sufficient [6–9].

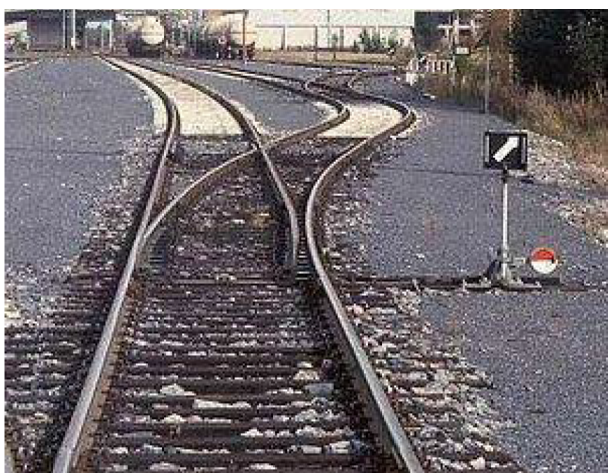


**Figure 1.** Shunting system for railway channels.



**Figure 2.** Currently used motorization for the shunting system.

## 3. Design and FEA of the LSRM

For moving the intermediate junction, 2 conditions must be satisfied. First, a displacement of 20 cm is required and second, a linear force equal to 4 kN is necessary. Based on these 2 requirements, an analytical design

combined with the FEM is carried out in order to determine the geometrical parameters of the proposed actuator. Figure 3 shows a 3-dimensional (3D) view of the proposed double-stator LSRM with 4 phases, where the excitation windings are located on the laminated structure of the stator. The mobile part (the translator) is placed in a position such that the left extreme phase is excited. If the left medium phase is excited, the translator movement will be towards the left. Otherwise, if the right extreme phase is excited, the mobile part movement will be towards the right [8]. The translator is the part coupled to the railway channels. The displacement of 20 cm segmented on 8 steps seems a good choice for positioning the intermediate rail. Hence, the step of the proposed actuator is given by:

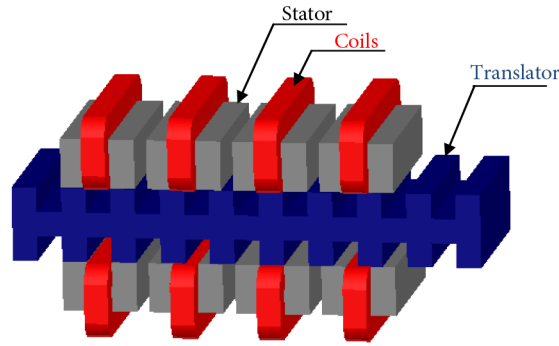


**Figure 3.** 3D view of the double-stator LSRM.

$$z_m = \frac{20}{8} = 2,5cm. \quad (1)$$

To assure the reversibility and the regularity of operation in step mode, 2 conditions must be satisfied. On one hand, the use of equal tooth widths on the mobile part and on the stator is indispensable. On the other hand, the slot width must be equal to the tooth width. Hence, for the proposed actuator, the tooth and slot widths are given by:

$$a = b = 2z_m. \quad (2)$$

The tooth pitch  $\lambda$  is calculated using the following expression:

$$\lambda = a + b. \quad (3)$$

To guarantee a regular step, a nonmagnetic material must be inserted between the various stator modules. Moreover, the operation principle requires that only one stator phase can be aligned with the mobile teeth when it is supplied. In addition, if the teeth of the active modules are aligned with the teeth of the mobile part, the teeth of the other stator modules must be shifted in order to generate a tangential force to move the mobile part [6]. The nonmagnetic separation  $c_0$  must verify the following expression:

$$|c_0 - a| = z_m. \quad (4)$$

Considering an allowable length for the LSRM, the nonmagnetic separation is fixed by:

$$c_0 = \frac{a}{2} = 2,5cm. \quad (5)$$

The air gap is selected so as to guarantee a maximum force and taking into account the mechanical construction difficulties. The slot depth is selected so as to place the stator windings. The main dimensions of the actuator

are shown in Figure 4, which provides a view of an elementary portion of the LSRM. The mechanical and electrical parameters of the actuator obtained after the analytical design are summarized in Table 1.

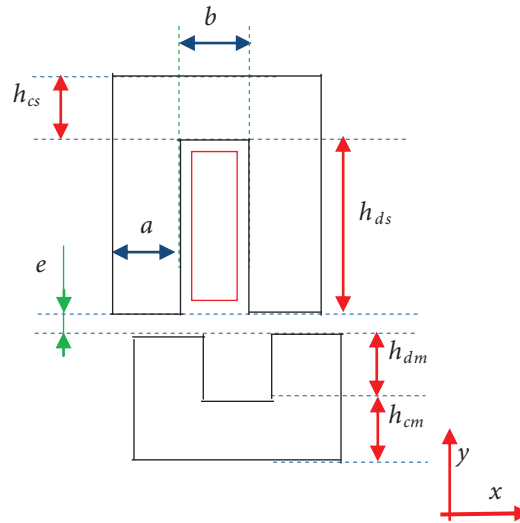


**Figure 4.** The main dimensions of the actuator.

**Table.** LSRM design specifications.

	Symbol	Values
Tooth width	$a$	5 cm
Slot width	$b$	5 cm
Phase separation	$c_0$	2.5 cm
Air gap width	$e$	2 mm
Step size	$z_m$	2.5 cm
Motor thickness	$L$	35 cm
Slot depth	$h_{ds}$	5 cm
Translator pole length	$h_{dm}$	5 cm
Stator cylinder head	$h_{cs}$	5 cm
Mobile cylinder head	$h_{cm}$	5 cm
Current excitation		4 A
Turns per phase		2000

The evaluation of the LSRM electromagnetic characteristics is based on a numerical field analysis by the FEM using Maxwell-2D. No complicated geometrical form is presented in the proposed actuator. Hence, a 2D FEA is considered to be sufficient and gives satisfactory results. The ferromagnetic material used in the FEM simulation is the steel that constitutes the material of the stator and the mobile construction. The nonlinear flux density and field strength (BH) curve of the used steel is given in Figure 5. The phase excitation is given as 8000 AT as a magnetomotive force. In fact, each winding has 2000 turns and the excitation current is considered to be 4 A.

The computational domain is represented by a cross section of the machine and the actuator's regions are meshed, as shown in Figure 6. Considering the great importance of the FEM results, the density of the mesh elements must be sufficient. However, a great number of elements increase the computation time. Hence, the mesh is a choice, taking into account the necessity of the accurate results and an acceptable computation time. Considering the magnetostatic field, the governing differential equation to be solved in the 2D FEM is:

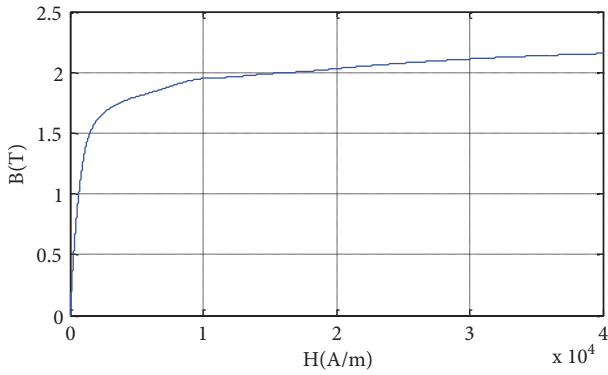


**Figure 5.** The BH curve of the ferromagnetic material (steel).

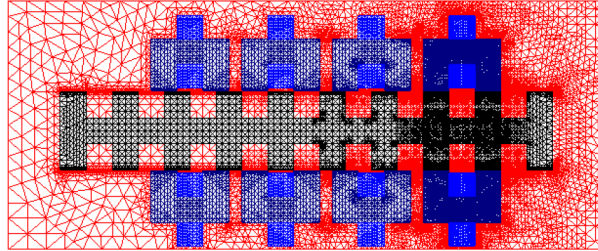


**Figure 6.** Mesh of the double-stator LSRM.

$$\frac{\partial}{\partial x} \left( \frac{1}{\mu} \frac{\partial A_z}{\partial x} \right) + \frac{\partial}{\partial y} \left( \frac{1}{\mu} \frac{\partial A_z}{\partial y} \right) = -J_z, \quad (6)$$

where  $A_z$  is the vector potential,  $\mu$  is the magnetic permeability, and  $J_z$  is the current density. The force generated to move the translator in the direction of the displacement (x-axis) is given by [4]:

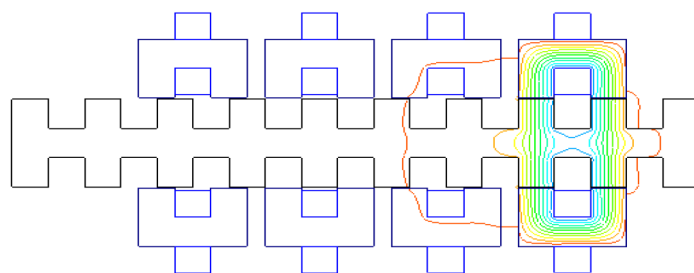
$$F(i, x) = \frac{\partial W'(i, x)}{\partial x}, \quad (7)$$

where  $W'$  is the total magnetic coenergy of the system, calculated as:

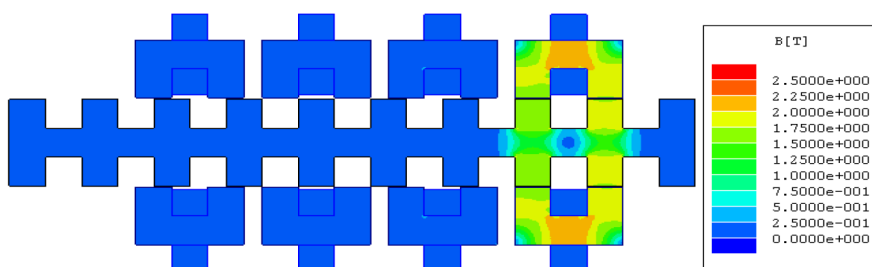
$$W'(i, x) = \int_V ( \int B dH ) dV. \quad (8)$$

Hence, the FEM software computes the magnetic potential with the aim of computing the magnetic coenergy and the propulsive force. To verify certain previously defined requirements such as the distribution of the magnetic field on the actuator structure, the first step of the analysis is to plot the magnetic field distribution. When the active coil, A, is fed by a current of 4 A, the flux lines and the magnetic field distribution in the aligned, intermediate, and unaligned positions are presented, respectively, in Figures 7, 8, and 9. The aligned position corresponds to the mobile teeth aligned with those of the stators'. In this position, the flux lines produced in the stator are canalized into the mobile part. Consequently, the magnetic flux density is maximum due to the neglected dispersion flux in these positions. The maximum flux density is approximately 2 T, as in Figure 7.

When the mobile keeps an intermediate position, as in Figure 8, the dispersion flux increases and the magnetic field distribution shows a reduction in the induction in both the mobile and the stator. However, a great flux density is noted on the overlapping regions due to the accumulation of the flux line distribution in those regions. Indeed, in this position, the inductance takes an intermediate value and the stator tends to move the mobile part to an equilibrium position. Hence, the force is roughly maximum in this position. Figure 9 shows the stator teeth unaligned with the mobile slots. In this position, the dispersion flux increases and the magnetic flux density decreases in both the mobile and the stator. Consequently, the inductance takes its minimum value in the unaligned position.

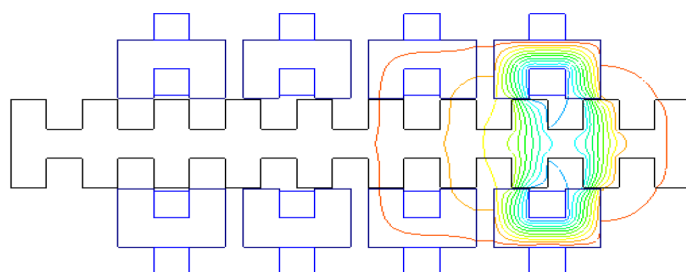


a. Flux lines distribution



b. Magnetic field distribution

**Figure 7.** Fully aligned position.



a. Flux lines distribution

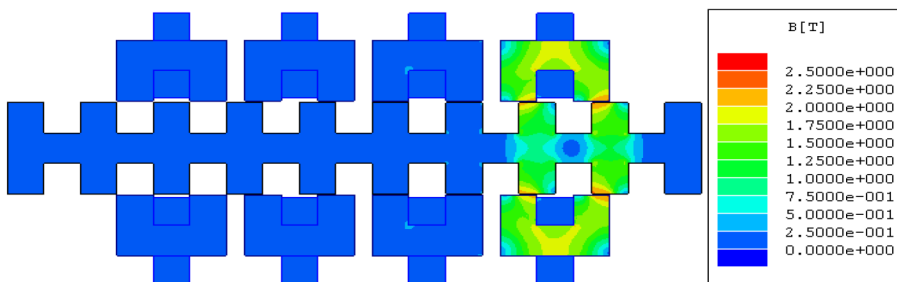


**Figure 8.** Overlapping position.

#### 4. Electromagnetic characteristics of the LSRM

To determine the performance of the proposed LSRM and to generate the magnetic characteristics, the procedure includes finding out the flux linkage and force characteristics versus the translator position and the applied

current. Hence, for evaluating the magnetic behavior, the translator of the LSRM is moved from an unaligned position to an aligned position for different current excitations. The aligned position is defined when the teeth of the stator are opposite those of the moving part. In this position, the flux linkage is maximum. However, in the unaligned position, the flux linkage is minimum. Figure 10 shows the flux linkage curves of phase A for different current excitations. For the same applied phase current, the flux is maximum when the translator is kept in the aligned position. For each position, the flux linkage increases with the excitation current. The nonlinear effect of the saturation begins at around 4 A. From this excitation, the flux increases gradually as the current increases. The curves of inductance with the translator positions for different current values, shown in Figure 11, also present an important conclusion about the magnetic behavior of the LSRM. The curve of inductance corresponding to the unaligned position is less due to the larger air gap in this position. At this position the phase inductance is at its minimum. In the aligned position, the phase inductance is at its maximum.

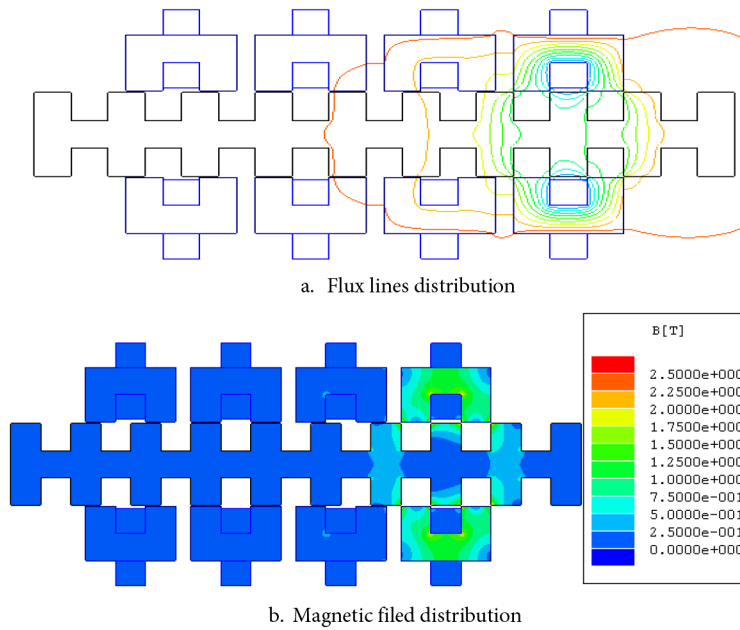


Figure 9. Fully unaligned position.

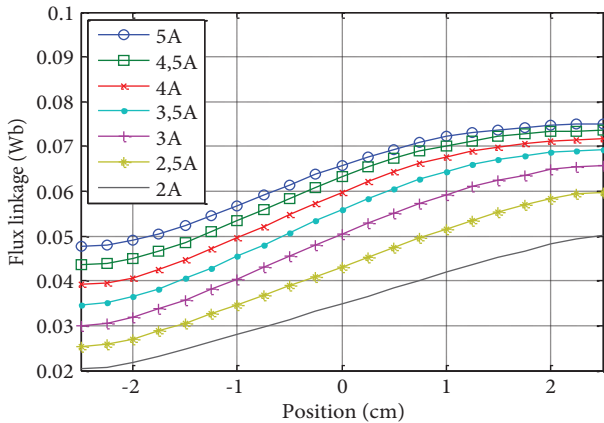


Figure 10. Flux linkage curves.

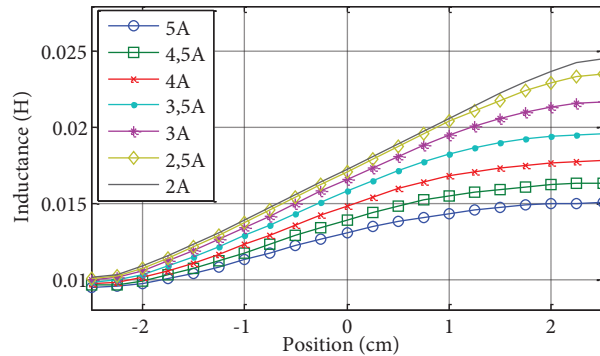
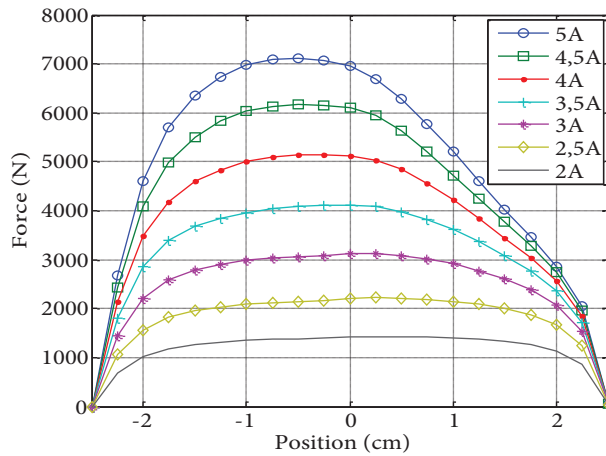


Figure 11. Inductance curves.



The components of the force are  $F_x$  and  $F_y$  in the x and y axes, respectively. The propulsion force  $F_x$  is needed for moving the translator. The attraction force  $F_y$  is much smaller than the propulsion force and is neglected. Indeed, each stator generates an attraction force in opposite directions; hence, the total attraction force in the y axis is neglected.

The curves of the propulsion force  $F_x$  with respect to the translator position calculated with the FEM are presented in Figure 12. The obtained results show that the propulsion force increases with the applied current. The forces at the aligned and unaligned positions are equal to 0. Moreover, these 2 positions correspond to the 2 equilibrium positions. The aligned position corresponds to the stable equilibrium position. However, the unaligned position corresponds to the unstable equilibrium position. The force curves confirm the nonlinearity of the force characteristics. Indeed, an asymmetrical force distribution is discovered along the mobile displacement. The distortion and the flatness of the force are noted for significant values of the current. On the intermediate position, the force is maximum, in order to allow the translator to move to the stable equilibrium position when the corresponding winding is excited. However, the maximum value of the produced force depends on the applied current. The nonlinearity of the force curves justifies the need for FEM analysis.



**Figure 12.** Propulsion force  $F_x$  vs. the translator position

Figure 13 shows the forces created by the 4 phases of the LSRM for the same applied current (4 A). The extreme phases develop a maximum force equal to 5145 N, whereas the maximum force produced by the central phases is 5060 N. This is due to the longitudinal end effect known in the linear electrical machines. The force value at the intersection of the curves is equal to 4300 N. This value corresponds to the start-up force. Hence, the proposed actuator is able to move a load force equal to 4000 N.

### 5. Modeling of the LSRM

The modeling of the LSRM is characterized by a high degree of difficulties because of the nonlinear electrical phase equation. In this paper, an advanced model is proposed; this model takes into account the nonlinearity of the electromagnetic characteristics with the magnetic saturation using the partial variation characteristics of the flux linkage presented in Figure 10 and the force characteristics presented in Figure 12.

Considering the equivalent circuit for each phase, the applied voltage  $U_j$  to a phase  $j$  ( $j = A, B, C, \text{ or } D$ ) is equal to the sum of the variation of the flux linkage added to the resistive voltage drop. Consequently, the electrical equation for each phase is given in [7,8,10,11]:



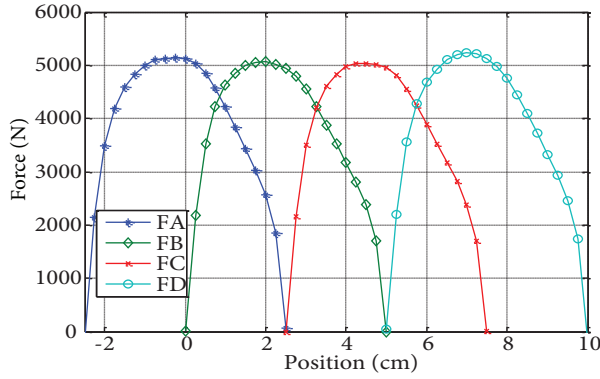


**Figure 13.** Propulsion forces of the 4 phases with 4 A.

$$U_j = R_j i_j + \frac{d\phi_j}{dt}. \quad (9)$$

The flux expression is dependent on the current excitation and the mobile part. Next, the expression of the flux variation can be written as:

$$\frac{d\phi_j}{dt} = \frac{\partial\phi_j}{\partial x} \frac{dx}{dt} + \frac{\partial\phi_j}{\partial i_j} \frac{di_j}{dt}. \quad (10)$$

Substituting the expression of the flux variation in Eq. (10) into Eq. (9), the equation of the applied voltage is expressed as:

$$U_j = R_j i_j + \frac{\partial\phi_j}{\partial x} \frac{dx}{dt} + \frac{\partial\phi_j}{\partial i_j} \frac{di_j}{dt}. \quad (11)$$

Hence, the time variation of the current is expressed by:

$$\frac{di_j}{dt} = \frac{1}{\frac{\partial\phi_j}{\partial i_j}} \left[ U_j - R_j i_j - \frac{\partial\phi_j}{\partial x} \frac{dx}{dt} \right]. \quad (12)$$

Eq. (12) shows the necessity of the flux characteristics for each phase for different currents versus the translator position, in order to complete the modeling of the actuator. Having obtained the flux curve, the partial derivative of the flux with applied current and the partial derivative of the flux with the mover position are calculated using the powerful MATLAB tool using the principle of partial derivation function.

When the excitation of the stator phases is maintained, the motion dynamics of the movable part of the motor is expressed by the following equation:

$$m \frac{d^2x}{dt^2} = F_x(x, i_j) - \xi \frac{dx}{dt} - F_0 \text{sign}\left(\frac{dx}{dt}\right) - F_r. \quad (13)$$

Finally, using Eqs. (12) and (13), the double-stator LSRM model is described by the following nonlinear differential equations:

$$\frac{di_A}{dt} = \frac{1}{\frac{\partial\phi_A}{\partial i_A}} \left[ U_A - R_A i_A - \frac{\partial\phi_A}{\partial x} \frac{dx}{dt} \right], \quad (14)$$

$$\frac{di_B}{dt} = \frac{1}{\frac{\partial\phi_B}{\partial i_B}} \left[ U_B - R_B i_B - \frac{\partial\phi_B}{\partial x} \frac{dx}{dt} \right], \quad (15)$$

$$\frac{di_C}{dt} = \frac{1}{\frac{\partial \phi_C}{\partial i_C}} \left[ U_C - R_C i_C - \frac{\partial \phi_C}{\partial x} \frac{dx}{dt} \right], \quad (16)$$

$$\frac{di_D}{dt} = \frac{1}{\frac{\partial \phi_D}{\partial i_D}} \left[ U_D - R_D i_D - \frac{\partial \phi_D}{\partial x} \frac{dx}{dt} \right], \quad (17)$$

$$m \frac{d^2 x}{dt^2} = F_x - \xi \frac{dx}{dt} - F_0 \text{sign}\left(\frac{dx}{dt}\right) - F_r. \quad (18)$$

### 6. Simulation results and discussion

Lookup tables based on the spline interpolation technique are used to find the intermediate parameter values of the flux linkage and the electromagnetic force. First, using Eq. (12), the value of the current for each phase is found for the values of the flux and mobile position. Next, the obtained value of the current is used to find the force created by the actuator. The block diagrams of the LSRM simulation package are presented in Figures 14, 15, and 16.

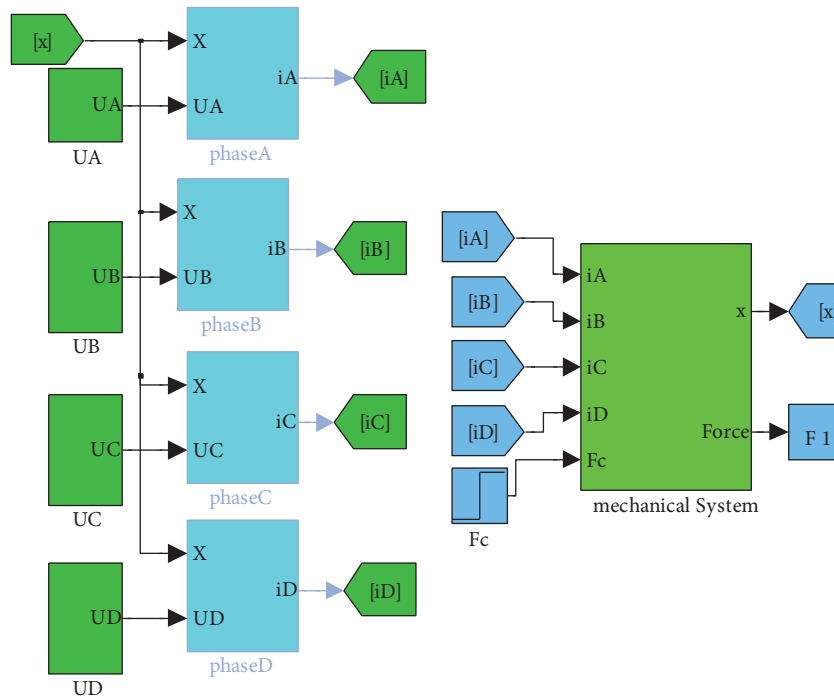


Figure 14. Nonlinear model of the LSRM.

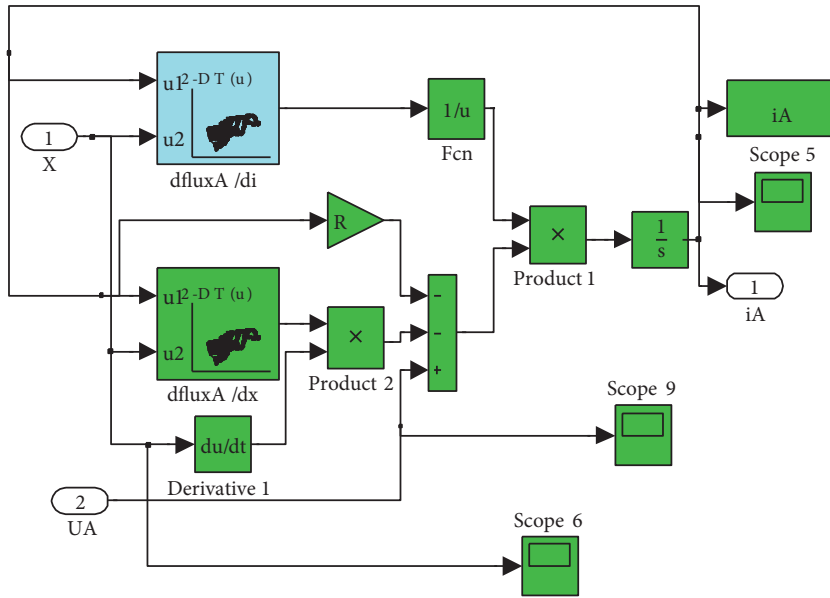


Figure 15. Simulation model of each phase.

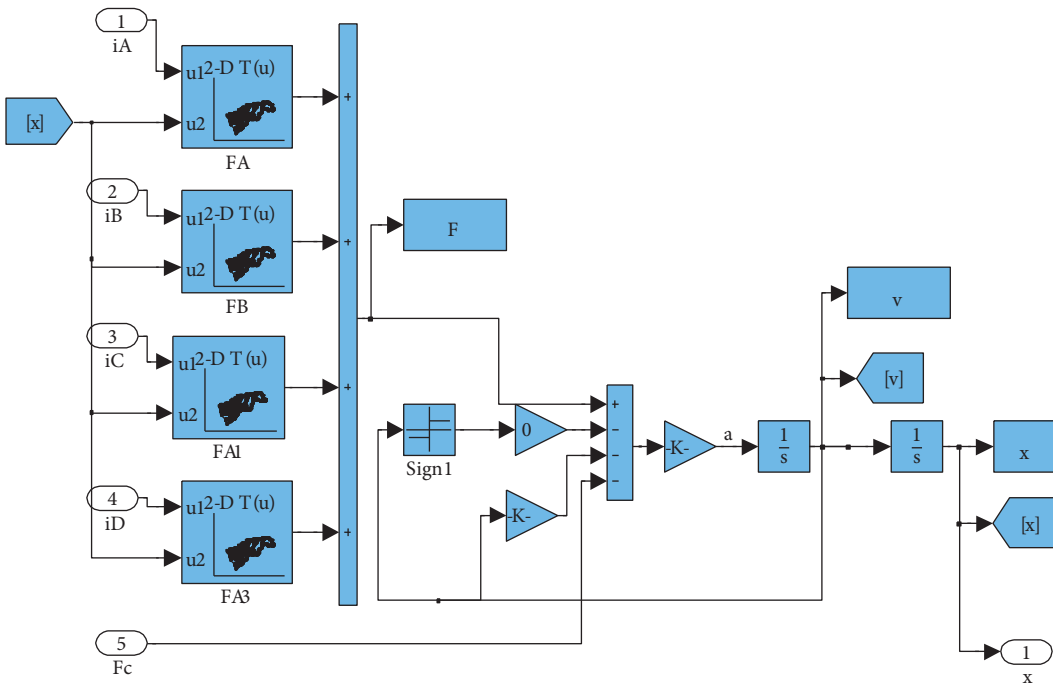
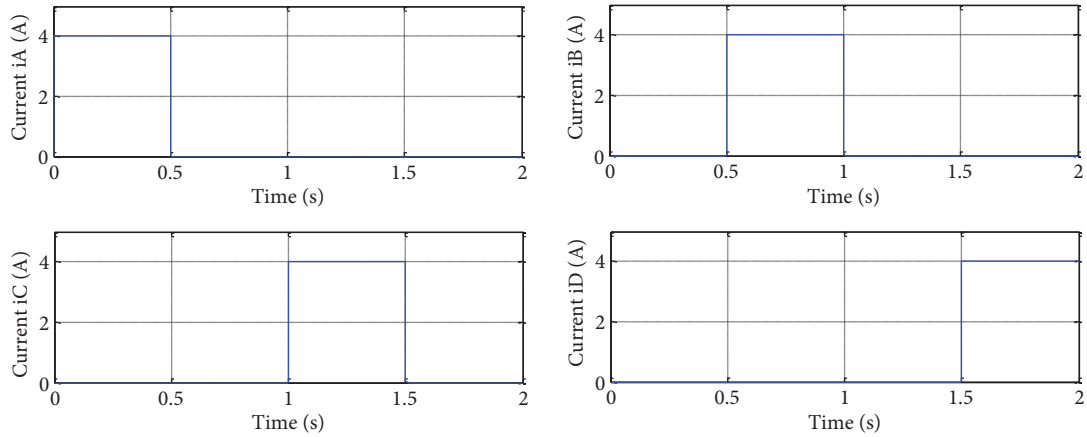
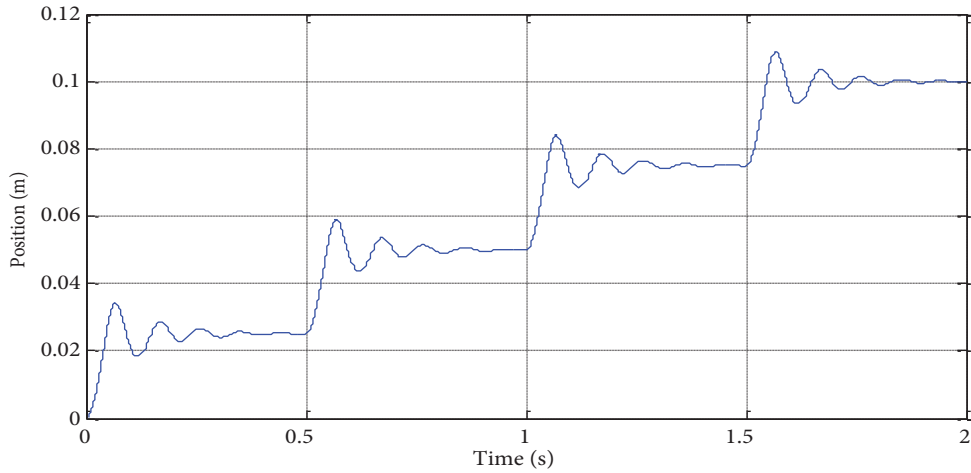


Figure 16. Simulation model of the mechanical equation.

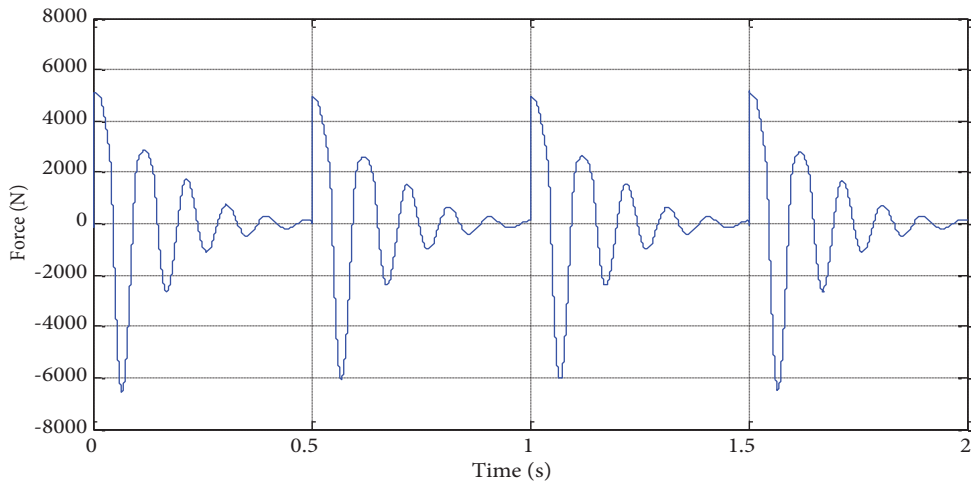
The purpose of the model including magnetic saturation is to verify the functioning of the actuator in order to elaborate some control techniques. Lookup tables based on the spline interpolation technique are used to find the intermediate parameter values of the partial derivative of the flux linkage and the produced force. The simulation results, shown in Figure 17, illustrate the workings in 4 successive full steps without a load.



a. Currents in different windings



b. Position response



c. Force response

**Figure 17.** Operation in 4 full steps.

The presented result shows that the excitation of phase A allows positioning of the translator on the first equilibrium position corresponding to 2.5 cm. For moving the translator to the next equilibrium stable

position, it is necessary to shut off the current in phase A and establish it in the next phase. To move the mobile part from the first position to the end position (displacement equal to 10 cm), phases A, B, C, and D must be excited successively. First, only phase A is excited. Second, phase B is excited, whereas phase A must be de-excited. In the third step, the current is shut off in phase B and established in phase C. In the final step, phase C is de-excited and phase D is excited. However, the shunting system requires a displacement equal to 20 cm; hence, the cycle of excitation of the 4 phases must be repeated twice, and this makes it possible to move the blades through a distance of 20 cm.

## 7. Conclusions

In order to improve the reliability and the maintainability of the shunting system for railway channels, this research work proposes to replace the current motorization with a new double-stator LSRM. In this paper, the design of the LSRM, based on the FEA, is made, and verified by simulation tests using the Maxwell tool. Indeed, the analysis of the actuator by finite element is carried out in order to establish the magnetic characteristics. A model for the LSRM, based on the FEA is proposed and verified by simulation tests using the powerful MATLAB-Simulink. The obtained results with the FEM and MATLAB/Simulink confirm the better performance of the proposed LSRM. The main future work may involve a compact design in order to obtain a high propulsion force. In the next stage, we must develop a new position control system for the actuator with a load.

## References

- [1] T.J.E. Miller, "Optimal design of switch reluctance motors", *IEEE Transactions on Industrial Electronics*, Vol. 49, pp. 1526, 2002.
- [2] J.J. Blakley, "A linear oscillating ferroresonant machine", *IEEE Transactions on Magnetics*, Vol. 19, pp. 1574–1579, 1983.
- [3] R. Krishnan, *Switched Reluctance Motor Drives Modeling Simulation Analysis Design and Applications*, Florida, CRC Press, 2001.
- [4] M. Jufer, *Electromecanique*, Presses polytechniques et universitaires romandes, Lausanne, 1995.
- [5] F. Daldaban, N. Ustkoyuncu, "Inductance estimating of linear switched reluctance motors with the use of adaptive neuro-fuzzy inference systems", *Gazi University Journal of Science*, Vol. 22, pp. 89–96, 2009.
- [6] E.M. Barhoumi, B. Ben Salah, "Design and simulation of a new LSRM for shunting the railways channels", *International Review on Modeling and Simulations*, Vol. 3, pp. 1072–1078, 2011.
- [7] E.M. Barhoumi, B. Ben Salah, "Modeling and control of a new LSRM for shunting the railways channels", *International Review on Modeling and Simulations*, Vol. 4, pp. 2012–2019, 2011.
- [8] E.M. Barhoumi, B. Ben Salah, "Modeling of a double stator LSRM based on finite elements analysis", *12th International Conference on Sciences and Techniques of Automatic Control and Computer Engineering*, pp. 761–769, 2011.
- [9] E.M. Barhoumi, M. Hajji, B. Ben Salah, "Design of a double stator LSRM with Improvements in the mobile structure", *1st International Conference on Renewable Energies and Vehicular Technology*, pp. 194–198, 2012.
- [10] M. Kant, J.P. Vilain, "Modélisation dynamique du moteur pas à pas", *Revue de Physique Appliquée*, Vol. 7, pp. 678–692, 1990.
- [11] B. Ben Salah, *Contribution à la conception, la réalisation, l'analyse et la commande de machines électriques*, Mémoire d'Habilitation Universitaire en Génie Electrique, ENIT-Tunisie, 2003.